The minimum Euclidean distance principle applied to improve the modulation diffraction efficiency in digitally controlled spatial light modulators

A. Lizana[1], A. Márquez[2,*], L. Lobato[1], Y. Rodange[1], I. Moreno[3], C. Iemmi[4], J. Campos[1]

[1]*Dept. de Física, Universitat Autònoma de Barcelona, Bellaterra, Spain*
[2]*Dept. de Física, Ingeniería de Sistemas y Teoría de la Señal, Universidad de Alicante, Alicante, Spain*
[3]*Dept. de Ciencia de Materiales, Óptica y Tecnología Electrónica, Universidad Miguel Hernández, Elche, Spain*
[4]*Dept. de Física, Fac. de Ciencias Exactas y Naturales, Universidad de Buenos Aires, Buenos Aires, Argentina*
**andres.marquez@ua.es*

Abstract: Digital addressing of the electrical signal in spatial light modulators, as it is the case in present liquid crystal on silicon (LCoS) displays, may lead to temporal phase fluctuations in the optical beam. In diffractive optics applications a reduction in the modulation diffraction efficiency may be expected. Experimental work is done characterizing the fluctuations amplitude and phase depth for three different digital addressing sequences. We propose a diffractive model to evaluate the modulation diffraction efficiency of phase diffractive optical elements (DOEs) in the presence of phase fluctuations. Best results are obtained for the most stable electrical sequence even though its phase depth is as small as 280°. The results show good agreement with the numerical calculation given by the model.

OCIS codes: (050.1970) Diffractive optics; (230.3720) Liquid-crystal devices; (230.6120) Spatial light modulators, (050.5080) Phase shift.

References and links

1. J. Turunen and F. Wyrowski eds., *Diffractive Optics for Industrial and Commercial Applications*, (Akademie Verlag, Berlin, 1997).
2. H. J. Coufal, D. Psaltis, and B. T. Sincerbox, eds., *Holographic Data Storage*, (Springer-Verlag, Berlin, 2000).
3. W. Osten, C. Kohler, and J. Liesener, "Evaluation and application of spatial light modulators for optical metrology," Opt. Pura Apl. **38**, 71–81 (2005).
4. S. T. Wu, and D. K. Yang, *Reflective Liquid Crystal Displays*, (John Wiley and Sons Inc., Chichester, 2005).
5. A. Hermerschmidt, S. Osten, S. Krüger, and T. Blümel, "Wave front generation using a phase-only modulating liquid-crystalbased micro-display with HDTV resolution," Proc. SPIE **6584**, 65840E (2007).
6. J. R. Moore, N. Collings, W. A. Crossland, A. B. Davey, M. Evans, A. M. Jeziorska, M. Komarčević, R. J. Parker, T. D. Wilkinson, and H. Xu, "The silicon backplane design for an LCOS polarization-insensitive phase hologram SLM," IEEE Photon. Technol. Lett. **20**(1), 60–62 (2008).
7. I. Moreno, A. Lizana, A. Márquez, C. Iemmi, E. Fernández, J. Campos, and M. J. Yzuel, "Time fluctuations of the phase modulation in a liquid crystal on silicon display: characterization and effects in diffractive optics," Opt. Express **16**(21), 16711–16722 (2008).
8. A. Lizana, I. Moreno, A. Márquez, E. Also, C. Iemmi, J. Campos, and M. J. Yzuel, "Influence of the temporal fluctuations phenomena on the ECB LCoS performance," Proc. SPIE **7442**, 74420G–1 (2009).
9. J. E. Wolfe, and R. A. Chipman, "Polarimetric characterization of liquid-crystal-on-silicon panels," Appl. Opt. **45**(8), 1688–1703 (2006).
10. A. Márquez, I. Moreno, C. Iemmi, A. Lizana, J. Campos, and M. J. Yzuel, "Mueller-Stokes characterization and optimization of a liquid crystal on silicon display showing depolarization," Opt. Express **16**(3), 1669–1685 (2008).
11. A. Lizana, A. Márquez, I. Moreno, C. Iemmi, J. Campos and M. J. Yzuel, "Wavelength dependence of polarimetric and phase-shift characterization of a liquid crystal on silicon display," J. Eur. Opt. Soc. – Rapid Pub. **3**, 08011 1–6 (2008).

#122442 - $15.00 USD Received 8 Jan 2010; revised 12 Feb 2010; accepted 1 Mar 2010; published 6 May 2010

12. A. Lizana, I. Moreno, C. Iemmi, A. Márquez, J. Campos, and M. J. Yzuel, "Time-resolved Mueller matrix analysis of a liquid crystal on silicon display," Appl. Opt. **47**(23), 4267–4274 (2008).
13. K. Lu, and B. E. A. Saleh, "Theory and design of the liquid crystal TV as an optical spatial phase modulator," Opt. Eng. **29**(3), 240–246 (1990).
14. J. L. Pezzaniti, and R. A. Chipman, "Phase-only modulation of a twisted nematic liquid-crystal TV by use of the eigenpolarization states," Opt. Lett. **18**(18), 1567–1569 (1993).
15. J. A. Davis, I. Moreno, and P. Tsai, "Polarization eigenstates for twisted-nematic liquid-crystal displays," Appl. Opt. **37**(5), 937–945 (1998).
16. A. Márquez, C. Iemmi, I. Moreno, J. A. Davis, J. Campos, and M. J. Yzuel, "Quantitative prediction of the modulation behavior of twisted nematic liquid crystal displays based on a simple physical model," Opt. Eng. **40**(11), 2558–2564 (2001).
17. P. Clemente, V. Durán, L. Martínez-León, V. Climent, E. Tajahuerce, and J. Lancis, "Use of polar decomposition of Mueller matrices for optimizing the phase response of a liquid-crystal-on-silicon display," Opt. Express **16**(3), 1965–1974 (2008).
18. I. Moreno, A. Lizana, J. Campos, A. Márquez, C. Iemmi, and M. J. Yzuel, "Combined Mueller and Jones matrix method for the evaluation of the complex modulation in a liquid-crystal-on-silicon display," Opt. Lett. **33**(6), 627–629 (2008).
19. I. Moreno, J. Campos, C. Gorecki, and M. J. Yzuel, "Effects of amplitude and phase mismatching errors in the generation of a kinoform for pattern recognition," Jpn. J. Appl. Phys. **34**, 6423–6432 (1995).
20. R. D. Juday, "Optical realizable filters and the minimum Euclidean distance principle," Appl. Opt. **32**(26), 5100–5111 (1993).
21. R. D. Juday, "Generality of matched filtering and minimum Euclidean distance projection for optical pattern recognition," J. Opt. Soc. Am. A **18**(8), 1882–1896 (2001).
22. I. Moreno, C. Iemmi, A. Márquez, J. Campos, and M. J. Yzuel, "Modulation light efficiency of diffractive lenses displayed in a restricted phase-mostly modulation display," Appl. Opt. **43**(34), 6278–6284 (2004).
23. A. Márquez, C. Iemmi, I. Moreno, J. Campos, and M. J. Yzuel, "Anamorphic and spatial frequency dependent phase modulation on liquid crystal displays. Optimization of the modulation diffraction efficiency," Opt. Express **13**(6), 2111–2119 (2005).
24. C. Soutar, S. E. Monroe, Jr., and J. Knopp, "Measurement of the complex transmittance of the Epson liquid crystal television," Opt. Eng. **33**(4), 1061–1069 (1994).
25. A. Bergeron, J. Gauvin, F. Gagnon, D. Gingras, H. H. Arsenault, and M. Doucet, "Phase calibration and applications of a liquid crystal spatial light modulator," Appl. Opt. **34**(23), 5133–5139 (1995).
26. Z. Zhang, G. Lu, and F. T. S. Yu, "Simple method for measuring phase modulation in liquid crystal television," Opt. Eng. **33**(9), 3018–3022 (1994).
27. D. Engström, G. Milewski, J. Bengtsson, and S. Galt, "Diffraction-based determination of the phase modulation for general spatial light modulators," Appl. Opt. **45**(28), 7195–7204 (2006).
28. S.-Y. Lu, and R. A. Chipman, "Interpretation of Mueller matrices based on polar decomposition," J. Opt. Soc. Am. A **13**(5), 1106–1113 (1996).
29. A. Márquez, C. Iemmi, J. Campos, J. C. Escalera, and M. J. Yzuel, "Programmable apodizer to compensate chromatic aberration effects using a liquid crystal spatial light modulator," Opt. Express **13**(3), 716–730 (2005).
30. A. Márquez, C. Iemmi, J. Campos, and M. J. Yzuel, "Achromatic diffractive lens written onto a liquid crystal display," Opt. Lett. **31**(3), 392–394 (2006).
31. M. S. Millán, J. Otón, and E. Pérez-Cabré, "Chromatic compensation of programmable Fresnel lenses," Opt. Express **14**(13), 6226–6242 (2006).
32. M. S. Millán, J. Otón, and E. Pérez-Cabré, "Dynamic compensation of chromatic aberration in a programmable diffractive lens," Opt. Express **14**(20), 9103–9112 (2006).

1. Introduction

Liquid crystal (LC) microdisplays have found a widespread range of applications in different areas such as diffractive optics [1], optical storage [2], or optical metrology [3]. In particular, liquid crystal on silicon (LCoS) displays have become the most attractive microdisplays for these applications due to their very high spatial resolution and very high light efficiency [4]. The digital addressing scheme (pulse width modulation) used in LCoS may lead to flicker in the optical beam [5,6]. The reason for the flicker is the limited viscosity of the LC molecules what allows them to follow each single pulse at a fraction. This means that the LC flickers around an average value what leads to a time dependent amplitude transmission. This may introduce temporal phase fluctuations [7,8] and/or a certain amount of depolarization [9–12] on the beam of light reflected by the LCoS. In fact, the digital addressing sequence, which is based in a pulse width modulation scheme, can be programmed. Shorter sequences offer the possibility of a higher repetition rate in a frame period, which has the effect of reducing the

#122442 - $15.00 USD Received 8 Jan 2010; revised 12 Feb 2010; accepted 1 Mar 2010; published 6 May 2010

flicker amplitude [5,6]. The number of addressable phase levels also reduces for shorter sequences, which should also be taken into account for some applications.

For the above mentioned applications and in particular for diffractive optics, it is very desirable to achieve a phase-only modulation regime, where a linear phase modulation up to 2π is produced versus the addressed gray level without coupled amplitude modulation. Many papers have demonstrated the usefulness of liquid crystal displays [13–16] and LCoS devices [17,18] to act as phase-only spatial light modulators. In general, all these papers consider the phase element addressed as a stable mask, without any source of phase fluctuation. To our knowledge, the effect on phase holograms of such phase fluctuations has not been analysed. This analysis is especially necessary in the case of present LCoS devices, since the digital addressing scheme used may lead to temporal fluctuations with a consequent degradation of their performance, as it will be the case in diffractive optics.

In addition to the temporal phase fluctuations, which will be analysed in detail in the present paper, there are a number of other defects which may deteriorate the performance of phase elements addressed onto a spatial light modulator [19]: 1) an amplitude modulation may be coupled to the phase modulation, 2) the phase modulation may not be linear with applied voltage, 3) the phase modulation depth may be less than 2π, and 4) the available phases may be limited to some quantized values. In diffractive optics these defects lead to a reduction of the modulation diffraction efficiency of the phase diffractive element. To solve these limitations it was found, in the context of filter design for pattern recognition, that the optimal solution is the Euclidean projection of each complex value to the closest available complex point in the modulation domain [20,21]. Later, several papers showed the application of this approach to the implementation of diffractive phase elements onto liquid crystal displays [19,22,23]. In all the cases the display was considered to show an electrical signal stable in time. It is now interesting to analyze the validity of the Euclidean projection approach taking phase fluctuations into consideration, and its usefulness to improve the modulation diffraction efficiency, defined as the intrinsic efficiency of the phase element disregarding other effects such pixelation or finite transparency of the display [22]. In particular, we need a calculation method in order to select the optimum digital electrical sequence with respect to the modulation diffraction efficiency.

The outline of the paper is as follows. In Section 2 we provide, for three different digital addressing sequences with different characteristics, experimental values for the temporal phase fluctuations and phase depth. In Section 3 we introduce the theoretical model and expressions that we propose to evaluate the performance of phase holograms and in particular of phase-only diffractive optical elements (DOEs) displayed onto spatial light modulators (SLMs) presenting temporal phase instabilities. In Section 4 we apply the theoretical model to calculate which electrical sequence provides more efficient phase elements. Both numerical and experimental values are given for the case of blazed gratings, showing that the saturated phase encoding technique derived from the minimum Euclidean principle provides the best efficiency for our device.

2. Temporal phase fluctuations: experimental characterization

In this paper we analyze a phase-only LCoS. It corresponds to an electrically controlled birefringence (ECB) LCoS display distributed by the company HOLOEYE. It is an active matrix reflective mode device with 1920x1080 pixels and 0.7" diagonal named the PLUTO Spatial Light Modulator (SLM). The pixel pitch is of 8.0 μm and the display has a fill factor of 87%. The signal is addressed via a standard DVI (Digital Visual Interface) signal. By means of the RS-232 interface and its corresponding provided software, we can perform gamma control to configure the modulator for different applications and wavelengths. Besides, different pulse width modulation (PWM) addressing schemes (digital addressing sequences) can be generated by the driver electronics [5], which can be programmed using the software included with the device. This will be applied in the present paper to characterize a

#122442 - $15.00 USD Received 8 Jan 2010; revised 12 Feb 2010; accepted 1 Mar 2010; published 6 May 2010

series of digital addressing sequences in terms of the phase values and temporal fluctuations they introduce in the beam of light.

In particular we will evaluate three digital addressing sequences whose configuration files are provided with the software and which can be loaded using this device driver software. They correspond to the configurations labelled as "18-6 default", "5-5 (1064)" and "5-5 (543)". The first number indicates the quantity of "equally weighted" bit-planes, and the second number the quantity of "binary" bit-planes [5]. This means that the sequence 18-6 is longer than the one corresponding for the sequence 5-5. In principle the shorter the sequence the smaller the flicker [5]. However, a larger sequence provides a larger number of possible phase levels: $(18 + 1) \times 2^6 = 1216$ for the sequence "18-6" and $(5 + 1) \times 2^5 = 192$ for the sequence "5-5". In principle, the sequences "5-5 (1064)" and "5-5 (543)" have been respectively optimized for the wavelengths 1064 nm and 543 nm. The voltage depth and gamma for the sequence 18-6 are also designed for the infrared. This means that for these wavelengths each of these two sequences should provide a phase depth of 2π radians, and quite a linear relation between phase value and gray level. Using these three different sequences we can evaluate different levels of flicker, of phase levels, and also of phase depth.

In order to be used as a phase-only device the incident light beam must be linearly polarized light along the director axis of the LCoS, which in the PLUTO device is along the horizontal axis of the laboratory reference system. Typically, two different types of techniques are used to measure the experimental phase modulation provided by liquid crystal devices: interferometric methods [24,25] or diffractive methods [26,27]. In Ref. [7] we demonstrated that interferometric methods are very adequate to obtain the average phase value, whereas diffractive methods are useful to obtain the instantaneous value for the phase. Another procedure to obtain the phase values is by means of the polar decomposition of the calibrated Mueller matrix for the LCoS [8,18,28]: from the retarder matrix in the polar decomposition the retardance values can be retrieved, which in the case of an ECB display and for linearly light along the director axis, correspond to the phase shift introduced in the light beam. Average or instantaneous phase values can be obtained depending whether the average or the instantaneous Mueller matrices are used. Next we show the results obtained for the average phase value and for the instantaneous phase value using the PLUTO LCoS display, for an incident wavelength of 633 nm from a He-Ne laser and for an angle of incidence of 2° (quasiperpendicular incidence). These measurements have been repeated for the three different digital sequences above specified.

The wavelength we use, 633 nm, does not correspond to any of the ones for which these sequences have been designed. In fact, this is not a problem. Sequences "18-6 default", "5-5 (1064)", designed for a longer wavelength, will provide a phase depth larger than 2π radians, which can be linearized and limited to 2π radians simply applying an appropriate look-up table. In the case of sequence "5-5 (543)" the phase depth will be shorter than 2π radians, what is also useful to evaluate the possibilities offered by the minimum Euclidean approach in case of limited phase depth. We also note that in multiwavelength applications [29–32] the spatial light modulator will provide 2π radians only for one wavelength of the set, while the rest will present different phase depth. In the rest of the paper we will refer to these sequences as #1 for "18-6 default", #2 for "5-5 (1064)", and #3 for "5-5 (543)".

In Fig. 1(a) we show the results obtained for the average phase value, using the retarder matrix obtained through the polar decomposition, and for the three sequences. We see that two of the sequences produce a phase modulation range larger than 360°: 520° and 480° respectively for the sequences #1 and #2 respectively. However, the phase depth for the sequence #3 is clearly smaller (about 280°). This could be expected since sequences the first two sequences are prepared for the infrared and the third one for the 543 nm wavelength.

#122442 - $15.00 USD Received 8 Jan 2010; revised 12 Feb 2010; accepted 1 Mar 2010; published 6 May 2010

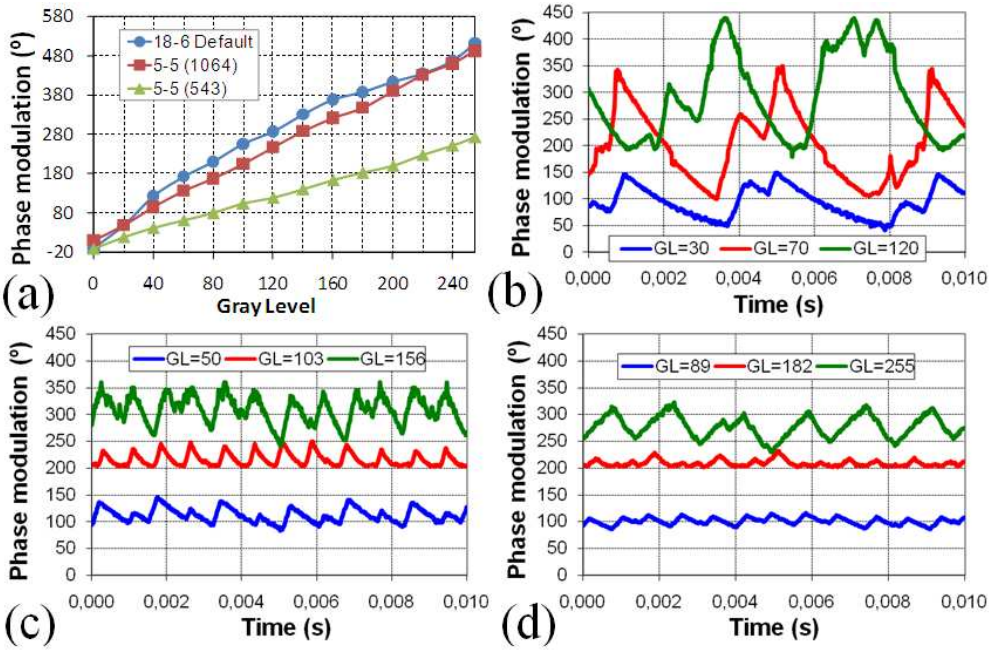

Fig. 1. Phase modulation values corresponding to the ECB LCoS display working as a phase-only device for 633 nm, and for the three electrical signal sequences. (a) Average phase. (b-d) Instantaneous phase for the sequences: (b) #1, (c) #2, and (d) #3.

We want to estimate the peak-to-peak phase fluctuation amplitude associated with each of the three addressing sequences. We choose to address phase values around 100°, 200° and 300° to sample the phase domain. In the case of the sequence #3 the maximum phase value we can address is 280°. From Fig. 1(a) we obtain to which gray levels these relative phase values correspond. We note that the zero phase reference value is taken at zero gray level where no temporal fluctuations exist in the reflected optical signal. In Figs. 1(b), 1(c) and 1(d) we show the instantaneous phase values, measured using the diffractive method [7], respectively for the sequences #1, #2 and #3. In the diffractive method a binary grating is addressed where one level correspond to the zero gray level and the other level correspond to the gray level associated with the phase value we want to reproduce. In each of the three graphs the blue, red and green curves represent the three phase values whose instantaneous magnitudes we want to measure. In the legend we have written the gray level addressed for the non-zero level in the binary grating, extracted from Fig. 1(a). It is evident that the fluctuations for the sequence #1, Fig. 1(b), are very large. They become much smaller for the sequences #2, #3, Fig. 1(c) and 1(d), corresponding to the shorter digital sequence ("5-5"). This is agreement with the general fact stated in literature [5,6] and commented in the Introduction Section: shorter sequences reduce the flicker amplitude. We note that the fluctuations repeat periodically. Among the two "5-5" configurations, configuration #3 shows a smaller fluctuation magnitude. In this case, we do not get full wave phase depth and we could think that it is a less efficient configuration. In Section 3, we will show a method which allows to increase the efficiency for phase DOEs displayed in a limited phase domain.

In Table 1 we show quantitative data for the magnitude of the phase fluctuations given in Figs. 1(b)-1(d). For each of the three sequences we show in each of the columns of the table the gray levels applied to the binary gratings, the average of the instantaneous phase value measured with this diffractive-based method, the peak-to-peak value for the temporal fluctuation of the phase, and the ratio (in percentage) between the peak-to-peak and the average phase value, which is what we will call fluctuation amplitude in the rest of the paper

#122442 - $15.00 USD Received 8 Jan 2010; revised 12 Feb 2010; accepted 1 Mar 2010; published 6 May 2010

unless otherwise stated. We see that the average phase value in each case is very close to the values extracted from Fig. 1(a) that we actually want to reproduce. With respect to the fluctuation amplitude we see that this value becomes even close to 120% for the first sequence, it is about 50% for the second sequence, and it is about 30% for the third. In each sequence this fluctuation amplitude changes with the average phase value in an interval about 20-30%. However there is not a monotonously increasing or decreasing tendency: as a first approximation we may consider a constant value for this magnitude, which is what we will apply in Eq. (2) in the theoretical development in Section 3.

Table 1. Values for the parameters characterizing the instantaneous phase signals shown in Figs. 1(b-d), measured with the diffractive-based method and for the three electrical sequences.

		Sequence #1	
Gray levels	Average phase (°)	Peak-to-peak value (°)	Fluct. amplitude (%)
0-30	95	107	113
0-70	206	249	121
0-120	290	260	90
		Sequence #2	
Gray levels	Average phase (°)	Peak-to-peak value (°)	Fluct. amplitude (%)
0-50	112	62	56
0-103	216	46	21
0-156	309	118	38
		Sequence #3	
Gray levels	Average phase (°)	Peak-to-peak value (°)	Fluct. amplitude (%)
0-89	101	30	29
0-182	209	30	14
0-255	277	92	33

3. Theoretical development

In Ref. [19] the effects were analyzed when an ideal phase-only diffractive element is displayed onto a display showing the typical constraints exhibited by liquid crystal SLMs: coupled amplitude modulation, non-linear phase modulation and phase dynamic range shorter than 2π radians. Using this model we can evaluate the amount of energy actually directed to the desired signal. This model also allows designing codification strategies which enhance this desired signal. At present, there are a series of strategies enabling for phase–only modulation with liquid crystal SLMs [13–18], and the residual non-linear phase modulation can be accounted for by using a proper look-up table. Thus, we can say that in general the first two constraints can be solved. However, in many situations the phase dynamic range available with liquid crystal devices is still shorter than 2π radians.

In Ref. [19] it was shown that, depending on the mapping scheme to implement the phase function onto the restricted phase-only domain, the modulation diffraction efficiency can be greatly enhanced. Figure 2 shows two possibilities for the implementation of the ideal phase-only function $h = \exp(i\varphi)$. The phase values available in the display are in the range $[0,\varepsilon]$, where ε is the phase depth. The diagonal line represents the correct matching between the designed phase φ and the displayed phase p. Model (1) in Fig. 2 represents a linear phase mismatching. A more efficient encoding is presented as the model (2) in Fig. 2, that we call a saturated mismatching encoding. This solution represents the perfect phase matching up to the maximum modulation depth $\varphi = \varepsilon$, while there is saturation for values $\varphi > \varepsilon$. Following the minimum Euclidean distance principle [20,21], we approximate each phase $\varphi > \varepsilon$ by the closest available phase. In general we concluded in Ref [19] that a continuous phase diffractive element with the saturated encoding (model 2 in Fig. 2) is more efficient that the implementation using the linear mismatch (model 1 in Fig. 2). We have used this saturated encoding to improve the efficiency of diffractive lenses [22], and to correct an anamorphic phase modulation effect caused by the electrical LCD addressing [23]. In this paper we extend

#122442 - $15.00 USD Received 8 Jan 2010; revised 12 Feb 2010; accepted 1 Mar 2010; published 6 May 2010

this model to the case when there are temporal phase fluctuations present on the phase-only element.

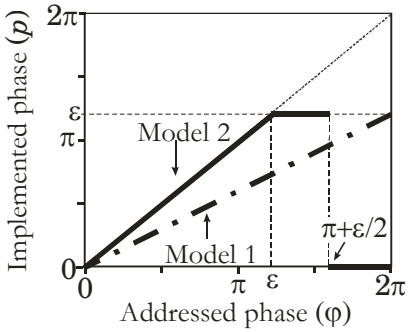

Fig. 2. Mapping scheme for the implementation of the linear mismatching encoding (Model 1) and the saturation mismatching encoding (Model 2).

Let $h(x,y) = \exp[i\varphi(x,y)]$ be the phase-only function to be displayed by the device. When this function is addressed to the phase-only display, in general the displayed phase values p will be different from the values addressed φ. The phase function implemented $m(x,y) = \exp[ip(\varphi(x,y))]$ is a periodic function of φ with periodicity 2π, therefore it can be expanded in Fourier series as given in Ref. [19].

$$M(\varphi) = A(\varphi)\exp(i\varphi') = \sum_{\alpha} G_{\alpha} \exp(i\alpha\varphi) \tag{1}$$

The interesting parameter is the hermitic product $|G_{\alpha}|^2$ for the coefficients in the expansion, which expresses the energy for each term. The desired phase function is exhibited by the first term of the Fourier expansion ($\alpha = 1$). The value for the coefficients associated with the other terms may become significant when there are defects in the phase reproduction. We note that the terms in the Fourier expansion can be spatially separated if a linear phase or a quadratic phase is added to the phase element [19].

Let us consider now which results may be expected when the values in the phase element exhibit a periodic temporal fluctuation, as it could be seen in Figs. 1(c)-1(d). The period of the pattern is much smaller than the typical integration time of the system (CCD camera) used in applications to acquire the optical signal reflected by the LCoS device. To ease the theoretical development we consider the following simplified model for the periodic evolution of the phase displayed $p(t)$ as a function of time t. First, we consider that the phase fluctuation can be modeled as a sawtooth profile in time with a period T. Second we consider that the amplitude of the fluctuation is proportional to the average value of the displayed $\overline{p}$, which may work as a first approximation as commented in the last paragraph in Section 2. Putting all this together we may describe the evolution of the displayed phase value along a period, between $0 \le t \le T$, as follows,

$$p(t) = \overline{p} + K\,\overline{p}\left(\frac{-1}{2} + \frac{t}{T}\right), \tag{2}$$

where K is a positive-valued constant which expresses the magnitude of the fluctuation. This is actually the fluctuation amplitude defined in Section 2 as the ratio between the peak-to-peak phase fluctuation and the average phase value. We note that in Eq. (2) it is not expressed in percentage. For $K = 0$ we would have no fluctuations and we would be in the situation described in Ref. [19,22]. When $K = 1$ we would have a peak-to-peak phase fluctuation equal to the average phase value $\overline{p}$.

#122442 - $15.00 USD Received 8 Jan 2010; revised 12 Feb 2010; accepted 1 Mar 2010; published 6 May 2010

Considering the fluctuation model in Eq. (2) and for the particular phase implementation schemes presented in Fig. 2 we can obtain the temporal evolution of the different coefficients $G_\alpha(t)$ in the Fourier series decomposition in Eq. (1). In the case when the linear mismatch is applied the important parameter to be introduced is the phase depth which is now fluctuating according to Eq. (2), thus,

$$\varepsilon(t) = \overline{\varepsilon} + K\,\overline{\varepsilon}\left(\frac{-1}{2} + \frac{t}{T}\right), \tag{3}$$

where $\overline{\varepsilon}$ is the average value for the phase depth. Then the linear mismatching encoding is expressed as,

$$m(\phi,t) = \exp\left[i\frac{\varepsilon(t)}{2\pi}\phi\right], \tag{4}$$

and we obtain that the coefficient for each Fourier term is given by,

$$G_\alpha(\overline{\varepsilon},K,t) = Exp\left[i\left(\frac{\overline{\varepsilon}}{2\pi} - \alpha + K\frac{\overline{\varepsilon}}{2\pi}\left(\frac{-1}{2} + \frac{t}{T}\right)\right)\pi\right]$$

$$\times\ \mathrm{sinc}\left(\left(\frac{\overline{\varepsilon}}{2\pi} - \alpha + K\frac{\overline{\varepsilon}}{2\pi}\left(\frac{-1}{2} + \frac{t}{T}\right)\right)\right), \tag{5}$$

where *sinc(x) = sin(πx)/(πx)*. Actually, the parameter related with the optical experiments is the time average of the energy for each Fourier term,

$$\eta_\alpha(\overline{\varepsilon},K) = \frac{1}{T}\int_0^T \left|G_\alpha(\overline{\varepsilon},K,t)\right|^2\,dt, \tag{6}$$

In the case of Eqs. (5) and (6), when there are no fluctuations, i.e. $K = 0$, we recover the result given in Ref. [19] when no fluctuations where considered,

$$\eta_\alpha(\overline{\varepsilon}) = \mathrm{sinc}^2\left(\frac{\overline{\varepsilon}}{2\pi} - \alpha\right) \tag{7}$$

We now consider the case when the saturated codification is used. We apply as the saturation value the average value for the phase depth $\overline{\varepsilon}$. Then, we have the following situation for the phase values p implemented as a function of the desired phase values φ,

$$p(\phi,t) = \begin{cases} \phi(t) & 0 < \phi \le \overline{\varepsilon} \\ \varepsilon(t) & \overline{\varepsilon} < \phi \le (2\pi + \overline{\varepsilon})/2 \\ 0 & (2\pi + \overline{\varepsilon})/2 < \phi \le 2\pi \end{cases} \tag{8}$$

where $\phi(t)$ corresponds to,

$$\phi(t) = \phi + K\,\phi\left(\frac{-1}{2} + \frac{t}{T}\right). \tag{9}$$

When using Eq. (8) we obtain that the coefficient for each Fourier term in the saturated encoding is given by,

#122442 - $15.00 USD Received 8 Jan 2010; revised 12 Feb 2010; accepted 1 Mar 2010; published 6 May 2010

$$G_\alpha\left(\bar{\varepsilon},K,t\right)=Exp\left[i\left(1-\alpha+K\left(\frac{-1}{2}+\frac{t}{T}\right)\right)\frac{\bar{\varepsilon}}{2}\right]\frac{\sin\left(\left(1-\alpha+K\left(\frac{-1}{2}+\frac{t}{T}\right)\right)\frac{\bar{\varepsilon}}{2}\right)}{\pi\left(1-\alpha+K\left(\frac{-1}{2}+\frac{t}{T}\right)\right)}$$

$$+Exp\left[i\left(1-\frac{\alpha}{2}+K\left(\frac{-1}{2}+\frac{t}{T}\right)\right)\bar{\varepsilon}\right]\frac{(-1)^\alpha-Exp\left[-i\,\alpha\,\frac{\bar{\varepsilon}}{2}\right]}{-i\,\alpha\,2\pi}$$

$$+\frac{1-(-1)^\alpha\,Exp\left[-i\,\alpha\,\frac{\bar{\varepsilon}}{2}\right]}{-i\,\alpha\,2\pi}. \tag{10}$$

In the case when no fluctuations are considered, $K = 0$, this expression converts into,

$$G_\alpha\left(\bar{\varepsilon},K=0,t\right)=Exp\left[i\left(1-\alpha\right)\frac{\bar{\varepsilon}}{2}\right]\frac{\bar{\varepsilon}}{2\pi}\operatorname{sinc}\left(\left(1-\alpha\right)\frac{\bar{\varepsilon}}{2\pi}\right)$$

$$+Exp\left[i\left(1-\frac{\alpha}{2}\right)\bar{\varepsilon}\right]\frac{(-1)^\alpha-Exp\left[-i\,\alpha\,\frac{\bar{\varepsilon}}{2}\right]}{-i\,\alpha\,2\pi}$$

$$+\frac{1-(-1)^\alpha\,Exp\left[-i\,\alpha\,\frac{\bar{\varepsilon}}{2}\right]}{-i\,\alpha\,2\pi}, \tag{11}$$

and the energy for the first term, $\alpha = 1$, which corresponds to the desired phase element is,

$$\eta_1\left(\bar{\varepsilon}\right)=\left\{\frac{\bar{\varepsilon}}{2\pi}+\frac{\sin\left(\bar{\varepsilon}/2\right)}{\pi}\right\}^2 \tag{12}$$

which corresponds to one of the results obtained in Ref. [22].

Next we show some simulations which exemplify what kind of results can be now obtained when applying this extended model including the effects of the temporal phase fluctuations. In Fig. 3(a) we plot the value for the energy of the first term in the Fourier expansion, which corresponds to the energy for the desired signal, as a function of the available depth for the phase modulation domain. This simulation has been plotted for 6 different situations given in the legend of the figure, where "Lin" and "Sat" stand respectively for linear and saturation mismatching encoding. The values in the legend correspond to the fluctuation full amplitude parameter K previously reported expressed as a percentage of the average phase value, i.e. $K = 1$ corresponds to a percentage of 100%. The curves are monotonously increasing with the phase depth, and the maximum value is achieved when the phase depth is 360°. It can also be seen that the energy for the first term diminishes with the increase in the fluctuation amplitude, thus degrading the performance of the phase-only element. We see that when no fluctuations exist the saturation encoding provides clearly a more energetic first term in comparison with the linear mismatching encoding. This is still true for a fluctuation amplitude of 50%, but in the case of 100% we see that the linear mistmatching provides a slightly larger energy than the saturation mismatching for a phase depth larger than 300°. This means than when the fluctuations are very large both encodings

#122442 - $15.00 USD Received 8 Jan 2010; revised 12 Feb 2010; accepted 1 Mar 2010; published 6 May 2010

may provide similar values and no advantage would be expected from applying the minimum Euclidean projection approach.

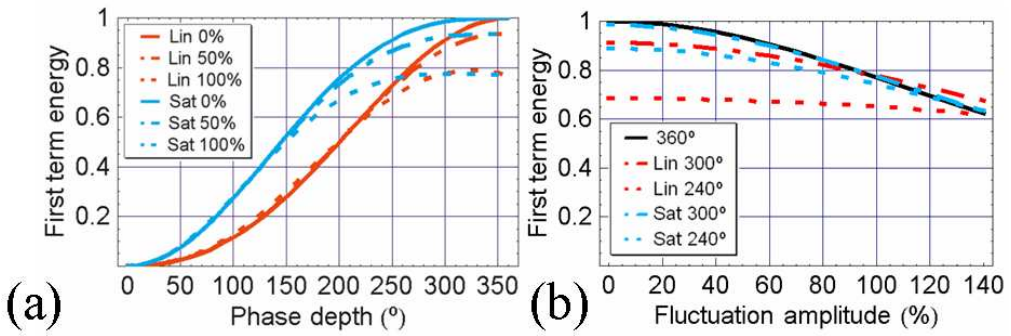

Fig. 3. Simulation for the energy for the first term $\alpha = 1$ and for the two mismatching encoding strategies: in (a) as a function of the phase depth and in (b) as a function of the fluctuation amplitude.

An alternative plot is given in Fig. 3(b) where the energy for the first term is represented as a function of the fluctuation amplitude. We show as a reference the energy obtained in the case when the available phase depth is 360°. The other curves correspond to the results obtained when the phase depth is restricted to 300° and 240°. We see that, for each value of fluctuation amplitude, the saturation encoding is in general more efficient than the linear mismatching, except for large values: we see that for a phase depth of 300°, when the fluctuation amplitude is larger than 90% the linear mismatching is providing slightly better results. We also see that even for such a reduced phase depth as 240° the energy provided by the saturated encoding is close to 90%, rather close to the curve obtained for the linear encoding for a phase depth of 300°. The saturated encoding for a phase depth of 300° provides the same efficiency as the linear encoding for a phase depth of 360°. Therefore, an important result extracted from this representation, which will emphasized in this paper, is that when using phase-only liquid crystal devices it may become more important to minimize the amplitude of the fluctuation than to maximize the phase depth. In general, a trade-off should be found, and the theory developed in this Section allows quantifying the goodness of this trade-off.

4. Numerical and experimental results

4.1 Numerical simulations: optimal sequence

A couple of conclusions could be drawn from the simulations presented in Fig. 3 in Section 3, in order to maximize the diffraction efficiency for the $\alpha = 1$ term (which is the desired term) in the Fourier expansion. We commented that when using phase-only devices not only the phase depth is important but also the fluctuation amplitude has a strong impact. Furthermore we demonstrated that using the saturation mismatching encoding we may maximize the diffraction efficiency to values close to the ideal even when the phase depth becomes significantly smaller that 360°. According to these ideas, and using the values expressed in Table 1, we want to calculate which of the three digital electrical sequences provides a more intense first order term. Two of the sequences provide the ideal phase depth of 360°, however their fluctuation amplitudes are about 120% (sequence #1) and 50% (sequence #2). The sequence #3 provides the smaller fluctuation amplitude, i.e. about 30%, but the phase depth is 280°, clearly smaller than 360°.

In Fig. 4 we show the numerical results obtained for the energy for the first term in the Fourier expansion. The vertical dashed lines indicate the fluctuation amplitudes of 50% and 120% associated respectively with the sequences #1 and #2. A series of curves have been

#122442 - $15.00 USD Received 8 Jan 2010; revised 12 Feb 2010; accepted 1 Mar 2010; published 6 May 2010

plotted, expressed in the legend. As a reference we show the curve corresponding to a phase depth of 360° (continuous red curve) which is plotted as a function of the fluctuation amplitude given in the *X*-axis in the plot. Together with this curve we show two horizontal lines corresponding to the energy value provided for a constant fluctuation amplitude of 30% and for a phase depth of 280°, which corresponds to the sequence #3. The two horizontal lines correspond respectively to the result obtained when applying the linear (long dash brown line) and the saturation mismatching encoding (short dash green line). We see that the energy value for the first term respectively for the sequences #1 and #2 is 0.69 and 0.93. For the sequence #3 the values are 0.84 and 0.94 respectively for the linear and for the saturation encoding. Therefore we obtain that the best option is to use the sequence #3 with saturated encoding, which provides an energy slightly larger than the one provided by the sequence #2. We remark this result: even though the phase depth is clearly smaller than 360°, a good value for the energy for the first term is obtained due to the lower fluctuation amplitude and to the use of the saturated encoding.

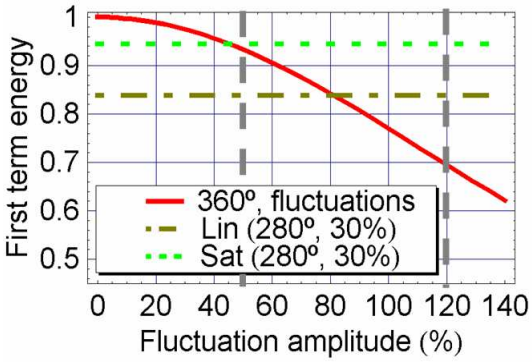

Fig. 4. Energy for the first term $\alpha = 1$ calculated for the values of the phase parameters corresponding to the three digital electrical sequences. We plot the energy values corresponding to a phase depth of 360° (continuous red curve) as a function of the fluctuation amplitude. In this curve the points with fluctuation amplitude values of 50% and 120%, indicated by the vertical lines, correspond to sequences #1 and #2. The two horizontal lines correspond respectively to the energy values obtained when applying the linear (long-short dash) and the saturated (short dash) encodings for the sequence #3, having a phase depth of 280° and a fluctuation amplitude of 30%.

4.2 Experimental results for a blazed grating

In this Section we want to verify experimentally the validity of the extended model proposed in Section 3. To this goal we address to the ECB LCoS a blazed grating and we measure the intensity diffracted to the zero and to the first diffracted orders. We note that these diffracted orders correspond to the terms $\alpha = 0$ and $\alpha = 1$ respectively in the Fourier expansion (Eq. (1)). We apply the three electrical sequences. In the case of the sequences #1 and #2 we limit the phase range between 0 and 360° and apply a look-up-table to produce a linear increment for the average phase value. For the sequence #3 the phase depth is already smaller than 360° and we apply both the linear and the saturation mismatching encoding. For the other two sequences, the linear phase is limited to the gray level providing an average phase of 360°, and the corresponding look-up table is applied to provide a linear phase. Thus the linear encoding is directly obtained. In all cases, the period for the grating is 16 pixels. This is a large enough number of pixels so that there is no need to consider the effect of the quantification of the phase levels. In this way we can apply the theory developed in Section 3, which is valid when the phase domain is continuous.

In Fig. 5 we show the measurements obtained for the intensity diffracted to the zero and first diffracted orders. Two radiometers are connected to the two channels of a digital oscilloscope in order to obtain instantaneous values. The intensity is normalized to the total

#122442 - $15.00 USD Received 8 Jan 2010; revised 12 Feb 2010; accepted 1 Mar 2010; published 6 May 2010

intensity reflected by the LCoS, which is measured in the zero order when a uniform screen is addressed. We show the results obtained when applying the sequences #1 in Fig. 5(a), #2 in Fig. 5(b), #3 with linear mismatching in Fig. 5(c), and #3 with saturation mismatching encoding in Fig. 5(d). We see that very large fluctuations are present for the sequence #1. On the contrary the diffraction efficiency for the first order is the highest and the signal the most stable for the sequence #3 with saturated encoding.

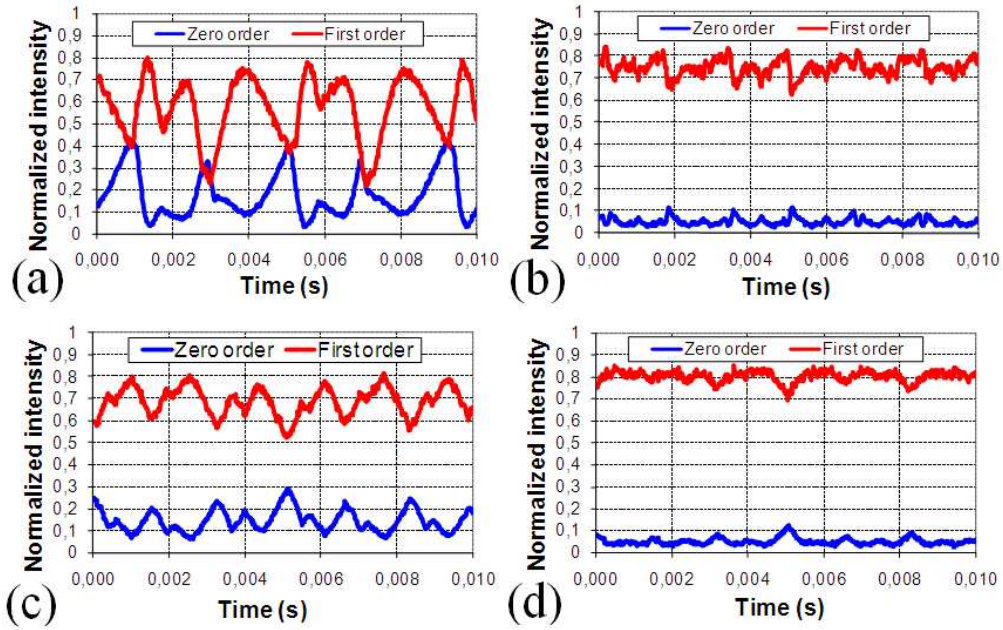

Fig. 5. Normalized intensity for the zero and first orders obtained when addressing a blazed grating and the following sequences and phase encoding schemes. (a) sequence #1, (b) sequence #2, (c) sequence #3 with linear mismatch, and (d) sequence #3 with saturated mismatch. The ECB LCoS is in the phase-only regime and it is illuminated with the wavelength 633 nm.

In Table 2 we show quantitative data obtained from the experiment in Fig. 5. We have also calculated the corresponding numerical values so that we can verify the prediction capability of the extended theory developed in Section 3. For the numerical simulation we consider the phase depths and the fluctuation full amplitudes already commented in the first paragraph in Section 4.1.

Table 2. Values for the parameters characterizing the instantaneous normalized intensities for the zero and the first diffracted orders produced by the blazed grating. Both experimental and numerical values are given.

		Experimental		Theoretical	
Sequence	**Normalized intensity**	**Order 0**	**Order 1**	**Order 0**	**Order 1**
#1	Average	0.18	0.57	0.11	0.69
	Std. deviation	0.10	0.14	0.15	0.24
#2	Average	0.05	0.75	0.02	0.92
	Std. deviation	0.02	0.04	0.02	0.06
#3 Linear encoding	Average	0.14	0.69	0.08	0.83
	Std. deviation	0.05	0.06	0.05	0.08
#3 Saturated encoding	Average	0.05	0.80	0.01	0.94
	Std. deviation	0.02	0.02	0.01	0.04

Let us analyze the average intensity values for the first order (columns 4 and 6). We see that both the experimental and the theoretical values agree with the tendency: the more

#122442 - $15.00 USD Received 8 Jan 2010; revised 12 Feb 2010; accepted 1 Mar 2010; published 6 May 2010

efficient results are obtained for the sequence #3 with saturated encoding, followed by #2, #3 with linear encoding, and #1. Actually we see that if an offset about 0.12-0.17 is substracted from the theoretical values, then the agreement between experiment and theory would be very good. We may think of various factors leading to this offset which diminishes the theoretical values. First, in the model we consider that the fluctuation amplitude is proportional to the average phase value but this is only a rough approximation as discussed in Table 1. Second, we consider that the ramp for the blazed grating is fluctuating in a synchronized manner, i.e. at any time there is a blazed grating and it is its phase depth what fluctuates. It is actually more likely that the different pixels composing the grating are fluctuating in a non-synchronized way: thus, at any time there are deviations from the ramp profile, leading to a smaller diffraction efficiency. This second possibility alone could probably explain this offset.

In the case for the average value for the zero order (columns 3 and 5), we also verify that the experimental and theoretical tendencies coincide. In this case the experimental values increase with respect to the theoretical ones. Let us now analyze the standard deviations associated with the temporal intensity fluctuations. We may see that the experimental and numerical values show a good agreement both for the zero and for the first diffracted order.

5. Conclusions

We have provided experimental measurements for the degree of the temporal phase fluctuations in the reflected optical beam given by LCoS displays. We have seen that depending on the format for the digital video signal these fluctuations may be reduced. According to literature shorter sequences should produce smaller fluctuations. We have used in the paper three different digital electrical sequences with different fluctuation amplitudes and one of them with a phase depth smaller than 2π radians. We have proposed a diffractive model to evaluate the efficiency of phase diffractive optical elements (DOEs) presenting phase fluctuations and reduced phase depth. Two phase encoding schemes are considered: linear and saturation mismatching. We demonstrate that saturation mismatching encoding, resulting from the minimum Euclidean projection onto the available values in the phase domain, provides more efficient phase elements unless the fluctuation amplitude becomes very large. The experimental and numerical results show a good agreement and validate the usefulness of the model. Using the model and applying the saturation mismatching encoding, we calculate which of the available electrical signal sequences provides more efficient blazed gratings. We find that for our specific LCoS unit the best results are obtained for the most stable electrical sequence even though its phase depth is as small as 280°. The presented approach is therefore a useful guide to operate LCoS devices for phase diffractive applications with improved diffraction efficiency, in spite of the losses caused by the phase fluctuation.

Acknowledgments

We acknowledge financial support from the Spanish Ministerio de Educación y Ciencia (grants FIS2009-13955-C02-01 and FIS2009-13955-C02-02) and from Generalitat de Catalunya (2009PIV 00051). C. Iemmi gratefully acknowledges the support of the Universidad de Buenos Aires and CONICET (Argentina).

#122442 - $15.00 USD Received 8 Jan 2010; revised 12 Feb 2010; accepted 1 Mar 2010; published 6 May 2010